phys. stat. sol. (a) **174**, 11 (1999)

Subject classification: 68.75.+x; S5

Intrinsic Stress Origin in High Quality CVD Diamond Films

I. VLASOV (a), V. RALCHENKO (a), D. ZAKHAROV (b), and N. ZAKHAROV (b, c)

(a) General Physics Institute, 38 Vavilov str., Moscow 117942, Russia
e-mail: vlasov@kapella.gpi.ru

(b) Institute of Crystallography, 59 Leninski Avenue, Moscow, Russia

(c) Max-Planck Institute of Microstructure Physics, Weinberg 2, D-06120 Halle, Germany

(Received March 25, 1999)

Anisotropic intrinsic stress in diamond films grown by microwave plasma chemical vapor deposition has been studied by Raman spectroscopy in conjunction with transmission electron microscopy (TEM). A series of films of 200 to 1400 μm thickness were analyzed. The confocal Raman spectroscopy has given detailed information on the stress distribution within individual grains of the films with a spatial resolution of a few microns. TEM analysis showed that the main defects of the films are sets of parallel microtwin lamella, starting from grain boundaries and ending inside the grains. Near-surface micro-Raman mapping revealed the preferable adjacency of compressive and tensile stress regions located on opposite sides of grain boundaries, while the depth analysis revealed stressed zones in different points of the bulk of these films. A mechanism of the extended (micron scale) stress generation due to formation of incoherent boundaries between coalescent crystallites is suggested using a model of edge dislocation structure of intergrain boundary.

1. Introduction

The knowledge of the mechanism of intrinsic stress generation in CVD diamond is of interest as the stress can reduce the mechanical strength of this material, moreover the stress relaxation can proceed via formation of defects which may degrade electronic and optical properties of diamond. Besides, the knowledge of the stress origin may shed light on the diamond growth process itself. Together with the traditional methods of crystal structure analysis the micro-Raman spectroscopy has become a basic technique for investigations of local intrinsic stress in CVD diamond [1 to 8]. For best CVD diamond films the Raman diamond linewidth can approach that of natural stones, $\approx$1.5 to 3 cm^{-1} (depending on the spectral resolution of apparatus). This allows, in particular, to observe a fine effect of diamond line splitting caused by anisotropic intrinsic stress [4,5,7,8].

In our previous works [7,8] high quality diamond films of the thickness 50 to 600 μm, grown in a microwave plasma reactor, have been analyzed by Raman measurements and incoherent boundaries between coalescent crystallites were considered [8] as a main source of the extended stress in polycrystalline films. In the present paper we used TEM and confocal micro-Raman analysis of the diamond films to discuss the mechanism of extended stress generation in more detail.

2. Experimental Procedure

The set of samples of 200 to 1400 μm thick diamond films was grown on a {100} silicon wafer of 57 mm in diameter by microwave plasma enhanced CVD in an ASTeX reactor

(5 kW power, 2.45 GHz) using a methane–hydrogen gas mixture. The deposition conditions were as follows: substrate temperature 700 to 720 °C, pressure 100 Torr, total gas flow rate 1000 cm^3/min, methane concentration 2%.

Raman spectra of free-standing films were recorded with a Raman spectrometer S-3000 (ISA/Jobin Yvon) using an Ar^+ laser at 514 nm wavelength and a confocal supplement as described elsewhere [7]. The microprobe provides a lateral spatial resolution of 2 μm, and a depth resolution of 5 μm upon analysis of surface layers, however, the depth resolution was somewhat poorer upon probing of the bulk.

For TEM examinations a high resolution microscope JEM 4000EX operated at 400 kV and a high voltage microscope JEOL 1MV were applied. To be transparent for electron beam a 200 μm specimen was thinned according to a three-stage process. First, the laser cut disk of 3 mm in diameter was mechanically polished from the growth surface to approximately 140 μm thickness to get rid of growth roughness. Then its back side was polished by a Gatan Dimple Grinder machine. In the third stage, the 70 μm thick specimen (in the thinnest point) was ion milled with Ar^+ at 6 kV and 10° incidence from both sides until a perforation occurred, and then the voltage was lowered to 4 kV and the ion milling was continued for 30 min. Thus the electron transparent areas were formed approximately in the middle of the films.

3. Results

3.1 Raman spectroscopy analysis

The growth surface of the films was examined by Raman microprobe analysing of the shape and position of the diamond Raman line, which is observed at 1332.5 cm^{-1}. A large number (of the order of 100) of grains was screened within each sample, and for a few selected grains a more detailed stress map has been obtained [7]. The magnitude of stress is estimated by using a linear dependence of the stress on the magnitude of the Raman line splitting. The splitting is measured as a distance between two maxima in the Raman line for resolved splitting. In case of unresolved splitting it is measured as difference between the widths of the asymmetrically broadened line and the narrowest line (2.8 cm^{-1}) in the stress-free regions. It was found that the mean level of stress estimated from this statistics decreases with increasing film thickness. For instance, for a 600 μm thick film the typical value of splitting was about 3 cm^{-1} (≈2 GPa by our estimate [7]), whereas for 1400 μm thick film it was about 1 cm^{-1} (≈0.7 GPa).

For bulk analysis the focus of the laser probe light descended vertically across the mechanically polished 1200 μm film, and a splitting of Raman line was observed at different depths from the surface. The in-depth analysis in the vicinity of the surface shows that two adjacent strain regions of opposite signs (tension and compression) are typically separated by the grain boundary. Figure 1 shows two sequences of Raman spectra taken at different depths along two vertical lines separated by a grain boundary. Both grains are stressed as revealed from asymmetric broadening of the Raman peak due to the peak splitting (unresolved here). However, the broadening direction is constant for one sequence (Fig. 1a), while it reverses for the second sequence recorded at the neighbor grain (Fig. 1b). The change of stress sign at a certain depth from the surface (Fig. 1b) can be assigned to an inclination of the grain boundary with respect to the film surface normal, so that the laser probe intersects the grain boundary upon profiling.

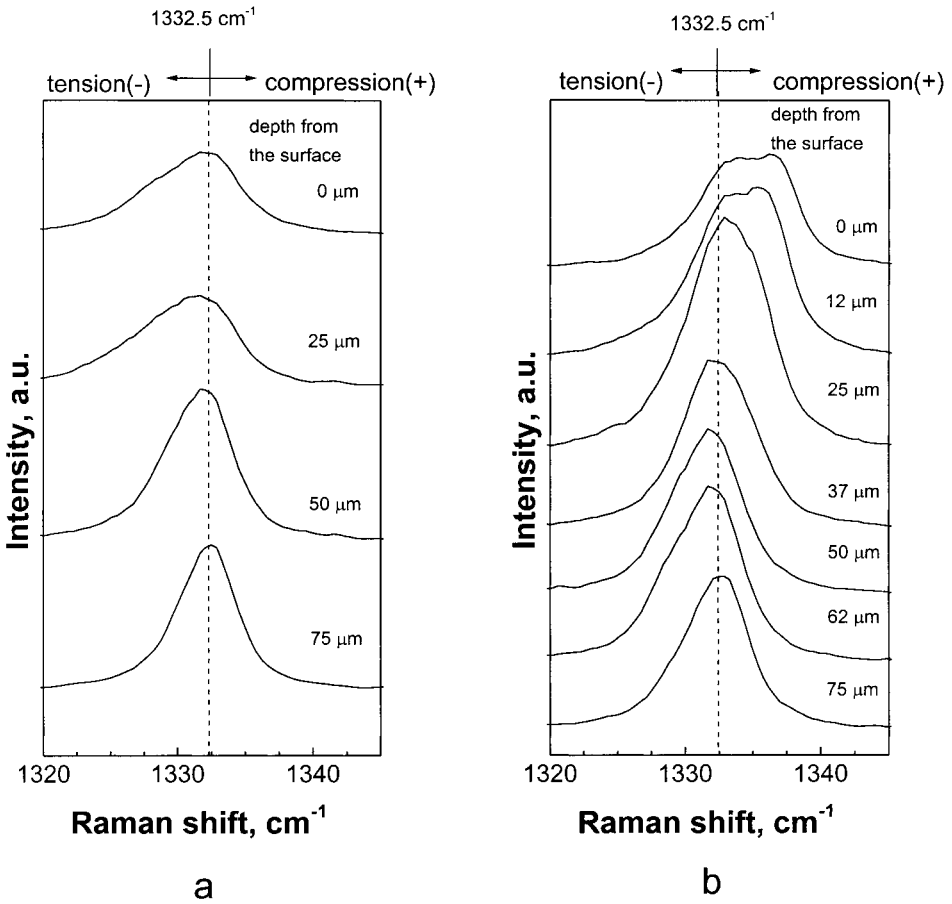

Fig. 1. Raman depth profiling along the straight trajectories extending from the surfaces of two adjacent strained grains. The starting points of the measurements are separated by a grain boundary, and their distance from the boundary is 5 μm. The stress keeps tensile in all measured points for one sequence of Raman spectra, i.e., diamond line splits to lower wave numbers with respect to the unstrained position of 1332.5 cm^{-1} (a), whereas the compression reverses to tension at the depth of 37 μm for another sequence (b)

3.2 Transmission electron microscopy analysis

The morphology of the diamond samples grown in conditions described above has been already investigated [7] and has shown preferable ⟨110⟩ growth direction of crystallites in the films. However, commonly it was impossible to get an image of the lattice for two adjacent grains simultaneously, that means that the grains are usually more than 2° misoriented.

The crystal structure reveals two typical groups of regions. The first one represents defect-free regions up to 5 μm in diameter that are compatible to lateral grain sizes of 10 to 30 μm. The second, predominant group of regions is characterized by rows of parallel microtwin lamellae starting preferably from certain parts of the grain boundaries and ending inside the grains. The typical distribution of the microtwins is demonstrated on bright field images in Fig. 2. The characteristic width of the lamellae is about

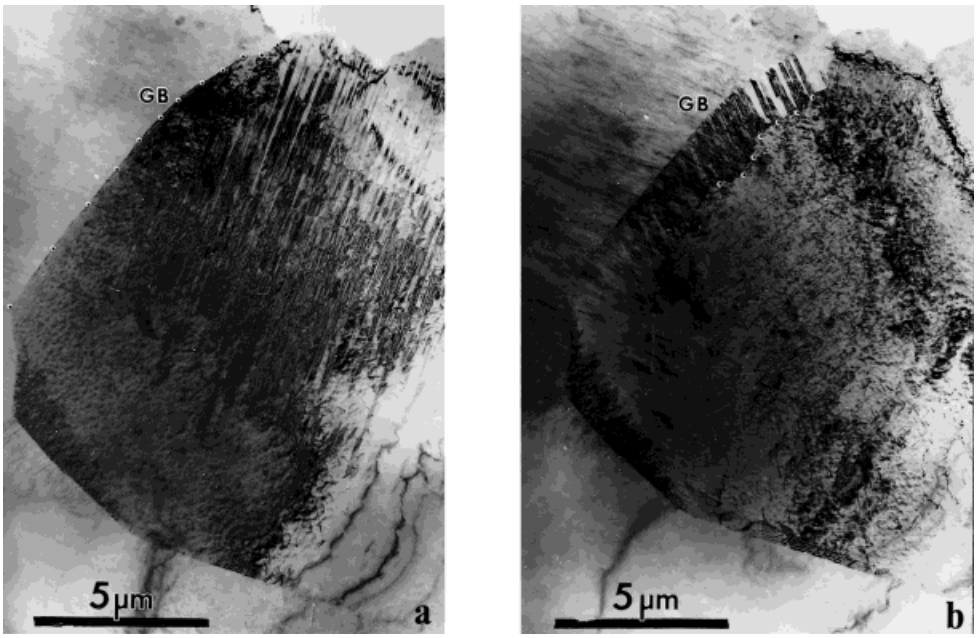

Fig. 2. Bright-field images obtained using the two-beam technique where one of the {220} diffracted beams is excited: a) parallel twins (in one of four {111} planes) starting possibly from grain boundary (GB) and ending inside the grain, b) twins in the second plane {111} starting from GB and ending (marked by small dots) on the first family of {111} twins

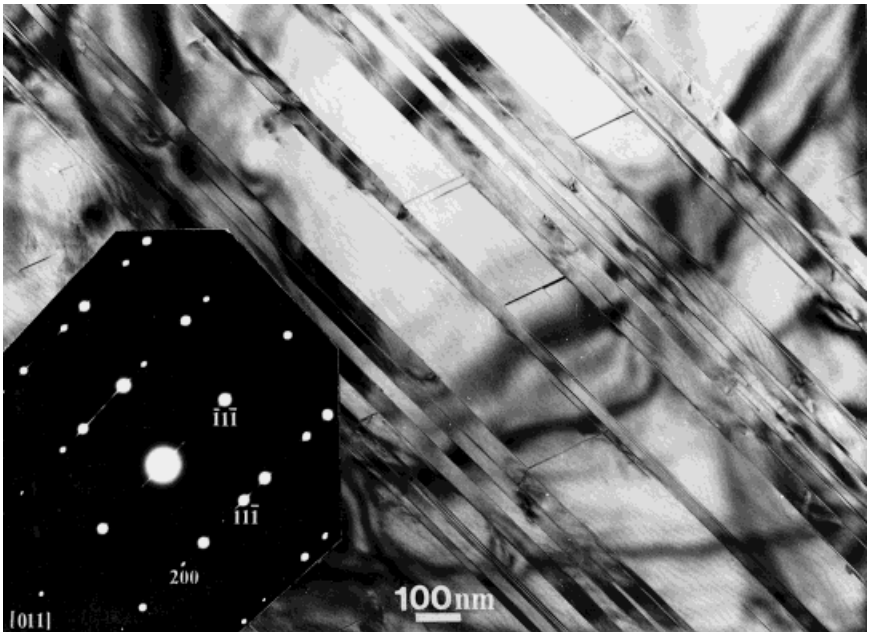

Fig. 3. Low magnification image of a parallel twin region. The diffraction pattern shows a twinning in one of the {111} planes (inset)

100 nm as seen in Fig. 3. Such multiple narrow twins are depicted by additional spots and streaks on the diffraction pattern. If formation of thin twin lamellae is assumed to be a mechanism which allows to reduce the inhomogeneously distributed strain in the crystal, the twins arrangement could give information on the location of the stress source. Once the lamellae are stretching preferably from the grain boundaries, this may indicate that the stress is generated in the grain boundaries. Besides the stress-induced twins, other twins are also arising during growth, when new atomic layer formation takes place in random points on (111) facets of growing crystallites and twinned and non-twinned nuclei are formed practically with equal probability [9].

4. Discussion

The extended stress in diamond can be caused by non-uniform distribution of defects and impurities depending on growth sectors within the individual crystals [10]. This possibility cannot be excluded; however, a few arguments exist against it for high quality CVD diamond. If the predominance of the "growth sector" stress is allowed for the films then:

1) all ⟨110⟩ oriented grains would have a similar distribution of strain regions within the grain surface. However, this is not the case: for some <110> oriented grains we did not observe the stress, while for others the number of stress regions varied between 1 to 5 within one grain [7];

2) the ⟨100⟩ oriented grains should show a certain stress, as it has been observed in [4,5], however, we did not detect any stress in this case. The stress is observed only in crystals with predominant orientation (⟨110⟩ oriented crystals in our work, and ⟨100⟩ oriented ones in [4,5]), i.e. for grains with relatively small misorientation;

3) the photoluminescence (PL) spectra characteristic for main defects should differ in stressed and non-stressed regions. However, we have got the same spectra for stress-free regions (Raman linewidth of 2.8 cm^{-1}), as well as for strained regions where the splitting broadens the line to 8 cm^{-1} (more than 3 GPa).

Therefore, we suggest that the process of coalescence of adjacent crystallites is possibly the main reason of the stress generation in diamond films of high quality.

4.1 Mechanism of stress generation in CVD diamond

Despite the preferable ⟨110⟩ orientation of the most growing crystals they can be slightly declined from growth direction and be arbitrarily rotated against each other in a film plane. In the case of low angle misorientation the meeting grains would try to accommodate to each other forming a single crystal, as it has been shown by TEM analysis for 2° misorientation [11]. The boundary between contacting grains can be of two types: coherent and incoherent. For simplicity only the case of two-dimensional misorientation will be discussed.

4.1.1 Coherent boundaries

The dislocation model of the boundary between two low-angle mismatching grains is shown in Fig. 4a [12]. The boundary consists of a set of edge dislocations placed on a distance of $D \approx b/\theta$ (where b is the length of Burgers vector, and θ the misorientation angle) from each other. The field of stress caused by individual dislocations is added up

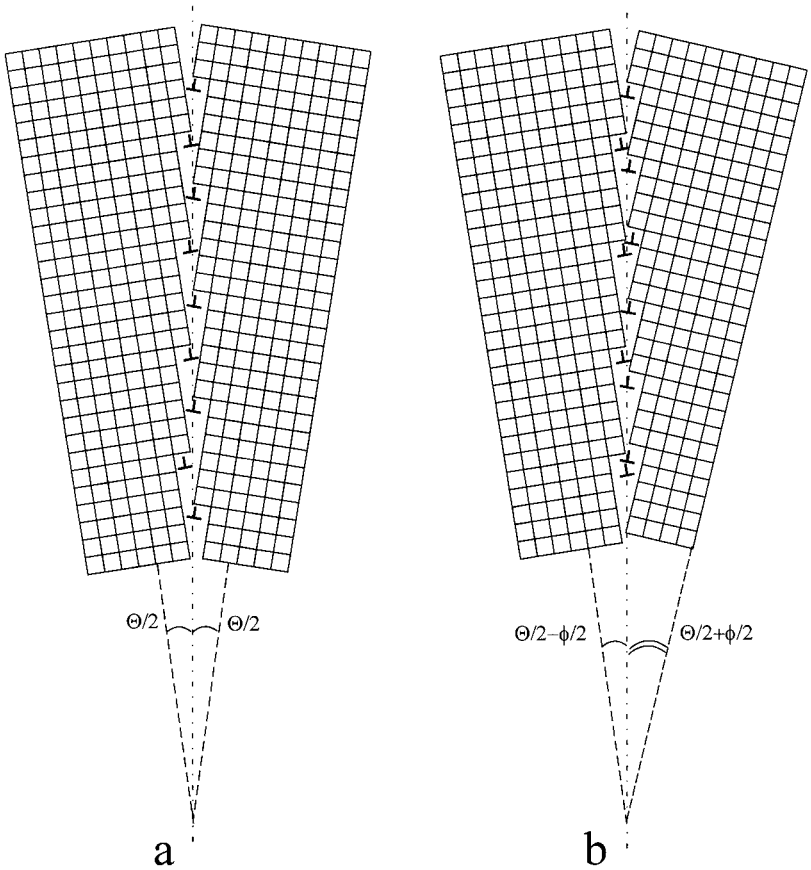

Fig. 4. Schematic illustration of the dislocation model of a) the coherent and b) the incoherent boundary between two coalescent crystallites

by a way that the resulting stress quickly decays over a distance D from the boundary without spreading in the bulk of the crystal.

4.1.2 Incoherent boundary

Now suppose that the boundary declines by a small angle $\varphi/2$ from the symmetric position (Fig. 4b), due to some reason. In this case an unequal number of atomic planes terminates at a common site of the coalescence boundary from opposite sides: $(\theta + \varphi)/2b$ planes intersect unit length of the boundary from one side, and $(\theta - \varphi)/2b$ planes from the other side. The dislocation distribution along the incoherent boundary differs from the former case by addition of an extra set of parallel dislocations with a repetition period b/φ from one side of the boundary. The stress field from the set of dislocations gives a macroscopic stress of grain interaction, resulting in a compression of one grain and tension of the other one [13]. A jump of the stress σ across the boundary can be roughly estimated by the expression for the stress field from a parallel set of disloca-

tions with alined Burgers vectors [13]:

$$\sigma \approx Eb_{\parallel}/h\,, \tag{1}$$

where E is Young's modulus, $b_{\parallel}$ the projection of Burgers vector on the boundary, h the distance between the dislocations. With $b_{\parallel} \approx b\theta$, and $h \approx b/\varphi$ we have

$$\sigma \approx E\theta\varphi\,. \tag{2}$$

Let us estimate possible values of the angles θ. Taking into account that $E \approx 1.05 \times 10^3$ GPa, a typical value of the stress is $\sigma \approx 1$ GPa, and that the minimal value of θ is achieved under $\theta = \varphi$, one finds $\theta_{\min} \approx 2^\circ$. For maximum observed stress of 9 GPa this angle is $\theta_{\min} \approx 6^\circ$.

Of course, the discussed model of interaction of coalescent grains is very simplified. Although the complex 3D interactions between grains take place during growth, the considered mechanism of stress generation could explain substantially the stress distributions observed.

There are many different opportunities for a particular grain to coalesce simultaneously with several crystallites. That is why we observed grains with different numbers of strained regions. A situation when the stress fields extending from the opposite boundaries are summed up in a center of the grain, is also possible, so a highly strained region can exist not only in the vicinity of boundaries, but also at the grain center [7].

5. Conclusions

Micro-Raman and TEM techniques were employed to thick CVD diamond films to determine the mechanism of high intrinsic stress formation in the films. The results obtained in previous works [7,8] and this one lead to following conclusions:

(i) High intrinsic stress is generated within micrometers at different points of the diamond films during the whole growth process. The magnitude of stress is decreasing with increasing film thickness. Compressive and tensile stresses commonly are adjacent, but separated by intergrain boundaries.

(ii) Predominant defects in high quality diamond samples are the rows of parallel microtwin lamellae starting from the boundary between the grains and ending off in the bulk of the grains.

(iii) High intrinsic stress in polycrystalline CVD diamond films can be explained by the dislocation model of incoherent boundary formation between coalescent crystallites.

Acknowledgements This work was partially supported by the European Commission, under Copernicus Contract No. ERBIC15CT970710, and by grant of Russian Foundation for Basic Research, No. 98-03-33217a.

References

[1] D. Schwarzbach, R. Haubner, and B. Lux, Diamond Relat. Mater. **3**, 757 (1994).
[2] N. C. Burton, J. W. Steeds, G. M. Meaden, Y. G. Shreter, and J. E. Butler, Diamond Relat. Mater. **4**, 1222 (1995).
[3] D. Rats, L. Bimbault, L. Vandenbulcke, R. Herbin, and K. F. Badawi, J. Appl. Phys. **78**, 4994 (1995).
[4] Y. von Kaenel, J. Stiegler, J. Michler, and E. Blank, J. Appl. Phys. **81**, 1726 (1997).

[5] S. SALVATORI, M. C. ROSSI, F. GALLUZZI, F. SOMMA, and R. M. MONTEREALLI, Proc. SPIE **3484**, 93 (1997).
[6] J. L. W. STEEDS, A. GILMORE, J. A. WILSON, and J. E. BUTLER, Diamond Relat. Mater. **7**, 1437 (1998).
[7] I. I. VLASOV, V. G. RALCHENKO, E. D. OBRAZTSOVA, A. A. SMOLIN, and V. I. KONOV, Thin Solid Films **308/309**, 168 (1997).
[8] I. I. VLASOV and V. G. RALCHENKO, Proc. SPIE **3484**, 103 (1997).
[9] J. MICHLER, J. STIEGLER, Y. VON KAENEL, P. MOECKLI, W. DORSCH, D. STENKAMP, and E. BLANK, J. Crystal Growth **172**, 404 (1997)
[10] T. R. ANTHONY and Y. MENG, Diamond Relat. Mater. **6**, 120 (1997).
[11] X. JIANG and C. L. JIA, Appl. Phys. Lett. **69**, 3902 (1996).
[12] C. KITTEL, Introduction to Solid State Physics, Izd. Nauka, Moscow 1978 (in Russian, p. 701).
[13] K. VAINSHTEIN, V. M. FRIDKIN, and V. L. INDENBOM, Modern Crystallography, Vol. II, Izd. Nauka, Moscow 1979 (in Russian, p. 318–325).
[14] M. H. GRIMSDITCH and A. K. RAMDAS, Phys. Rev. B **11**, 3139 (1975).